Shaping effects of sand flow channels on aeolian geomorphology – a case study of the Badain Jaran, Tengger, and Ulan Buh Deserts, northern China

Wentao Sun, Xin Gao [*], Jiaqiang Lei

State Key Laboratory of Desert and Oasis Ecology, Xinjiang Institute of Ecology and Geography, Chinese Academy of Sciences, 818 South Beijing Road, Urumqi 830011, Xinjiang, China
University of Chinese Academy of Sciences, Beijing 100049, China

ARTICLE INFO

ABSTRACT

Based on the interactions between mountains, we identified three sand flow channels in the Badain Jaran, Tengger, and Ulan Buh Deserts, northern China. We found that the height difference of the terrain in these areas provided favorable conditions for the transportation of sand. Owing to the venturi effect of their geomorphologies, airflow was compressed in these channels, and their wind regimes were strong and unimodal. Compared with the interior of the desert, the sand transport potential was relatively large in these areas, and westerly and northwest winds prevailed. We found that the wind accelerated in the sand flow channels, resulting in faster-moving dunes. The dune types that developed in these channels were relatively simple owing to the unimodal wind regimes; they mainly comprised barchan and transverse dunes. We also identified a transition landscape from barchan dunes to transverse, or complex dunes. Based on their sediment characteristics and the prevailing wind directions, we found that the sand flow channels provided a direct sand supply between the three deserts. The sand flow channels connected these independent deserts to an entire desert system. Similar sand flow channels can also be found in other deserts globally. Collectively, these sand flow channels reflect interactions between deserts.

1. Introduction

The formation and evolution processes of deserts are often closely associated with mountain plateaus (Zhu, 1980). From the global distribution of major deserts, where there is desert formation, there are generally high mountains around. Generally, high mountains prevent warm and humid airflows from deepening, thereby forming a relatively closed dry terrain. Impenetrable terrain can lead to something like the Fohn effect, where air sinks and heats up. The resulting warming and drying effects then accelerate the weathering of rocks, wind erosion, and the accumulation of wind-carrying materials (Yang et al., 2008), which in turn promotes the formation and development of deserts. Interactions between regional wind flow and topographic steering can strongly affect wind speed and sand transport (Schwarz et al., 2021).

For example, the Taklamakan Desert, which is located in the Tarim Basin of China, is surrounded by mountains on three sides. This directly affects the destruction and reconstruction of the zonal circulation in this area. Prevailing wind is blocked and results in unique wind system at the

edge of mountains or hills (Zu et al., 2005), thus shapes the distinct dune landscapes of the area. The Rub Khali Desert on the Arabian Terraces has high cliffs to the west and south, the Zagros Mountains to the east, and the Ad-Dahna Desert to the north. The area's occluded terrain makes it dry, as water vapor cannot penetrate deeply. This accelerates the weathering and erosion of the desert surface (Yang et al., 2008). Located in the middle of the Taklamakan Desert and west of the Hotan River, the Mazartagh Mountain blocks some of the prevailing easterly and northeasterly winds from blowing deep into the southwestern area of the desert. Therefore, the northern side of the mountain is affected by changeable topographic wind patterns, leading to the development of tall and dense pyramid dunes, while the south side of the mountain piedmont features many salt-alkali crusts (Yang and Lu, 1990). This shows that mountains that develop in the interior of a desert will also affect the evolution of the dune landform patterns.

Wilson (1971) estimated the natural wind erosion rate of the Sahara Desert and proposed that wind erosion mainly arose from alluvial river deposits. Therefore, rivers that originate in mountains have also been
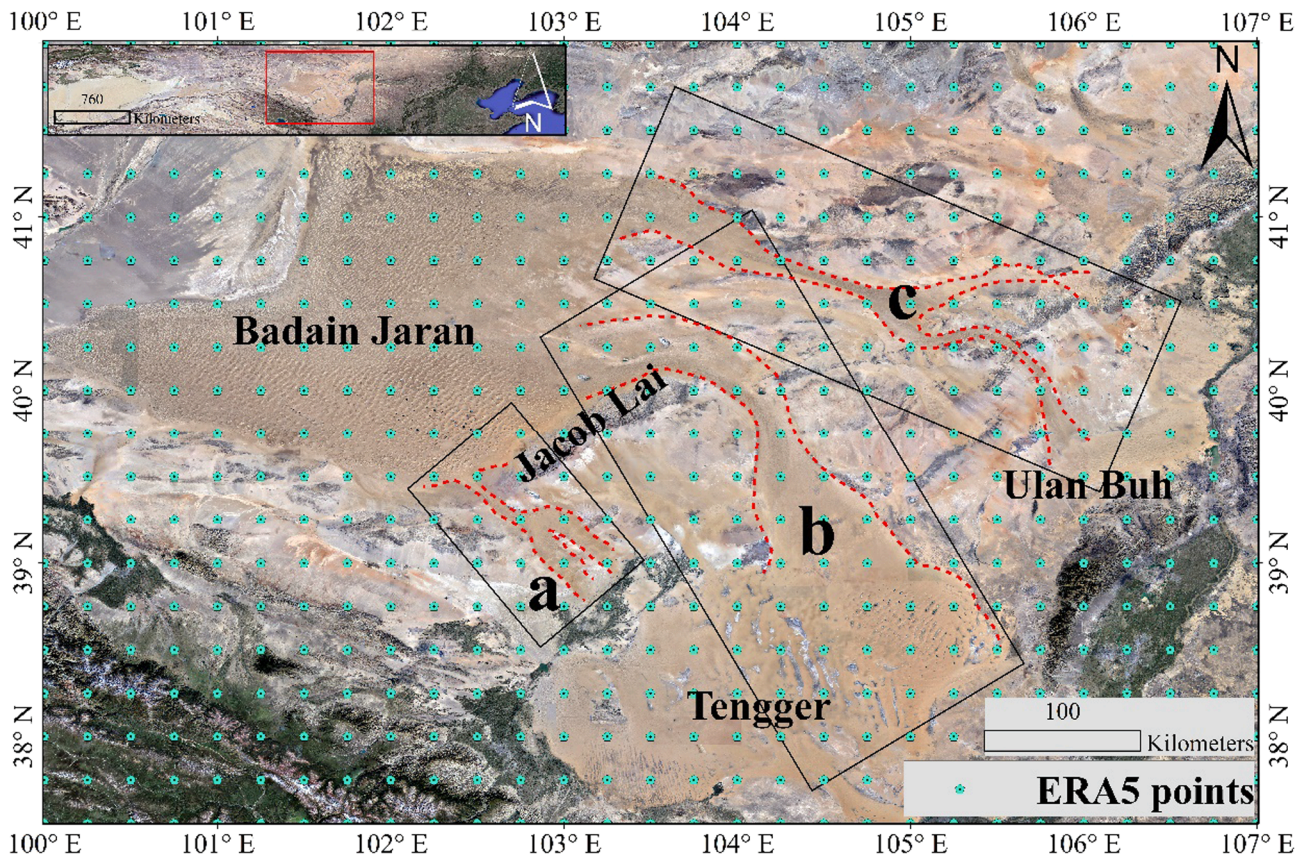

Fig. 1. Location of study area. Red dashed lines in black boxes (a, b and c) show locations of sand flow channels. Blue points show sample distribution of ERA5 data (temporal resolution = 1 h; spatial resolution = 0.25°×0.25°). (For interpretation of the references to colour in this figure legend, the reader is referred to the web version of this article.)

identified as essential sources of desert development; they can be considered to represent the skeletons and arteries that form deserts (Fedorovich, 1962; Yan et al., 2015). The geological units developed by rivers control the distribution patterns of deserts (Jin and Dong, 2001; Bullard and McTainsh, 2003; Draut, 2012). Thus, mountains, plateaus, and rivers play essential roles in shaping the landscapes of deserts. However, the unique topography produced by interactions between mountains is also an essential factor that affects the evolution of deserts.

Few studies have investigated sand flow channels, especially natural sand flow channels constructed by topographical differences between mountains. Gao et al. (2021) explained the contradiction between dune movement and sand flow path using morphological dynamics by studying reversed dunes in the Molcha River alluvial fan area, at the junction of the Tibetan Plateau and the Taklamakan Desert. However, this approach still focused on the morphodynamics of dune development.

Here, however, we mainly considered natural sand flow channels formed by interactions between mountains. The Badain Jaran Desert, Tengger Desert and Ulan Buh Desert in northern China have developed three typical sand flow channels due to the interaction between mountains. From a geomorphological perspective, we analyzed the wind regime, intensity, and direction of sand flow in these channels, investigated the distribution and movement rules of dunes, and explored the role of sand flow channels in shaping the desert system.

2. Study area and methods

2.1. Study area

The Badain Jaran Desert is located in the western part of the Alxa

Plateau, in the Inner Mongolia Autonomous Region of China; it contains the largest sandy mountains (>100 m) worldwide (Li et al., 2006). It is separated from the Tengger Desert by the Jacob Lai Mountain. The Ulan Buh Desert is located in the eastern part of the Alxa Plateau in Inner Mongolia, bordering the Yellow River in the east and the northern foot of the Helan Mountains in the south (Chun et al., 2007), adjacent to the Hetao Plain. Regarding its geological structure, the area comprises a piedmont sedimentary basin, with a dry climate, relatively high winds, and relatively little rain. By analyzing satellite images, we observed three obvious sand flow channels (Fig. 1).

2.2. Dataset

Reanalysis combines model data with observations from across the world into a globally complete and consistent dataset using the laws of physics. The European Centre for Medium-Range Weather Forecasts (ECWMF) was one of the earliest institutions to perform data reanalysis (https://www.ecmwf.int/). Olauson (2018) compared the modelling performance of ERA5 and MERRA-2 reanalysis data and found that ERA5 data had a higher correlation and the distribution and variation of hourly data were closer to the measured data. Meng et al. (2018) compared the data of 10 observation stations in Shandong, China and surrounding areas with ERA5 and ERA-Interim reanalysis data, and found that the assimilation data had a good correlation with the measured data. ERA5 data are more applicable than ERA-Interim data. Therefore, we selected ERA5 wind data (1979–2019) with a height of 10 m, a temporal resolution of 1 h, and a spatial resolution of 0.25°×0.25° to calculate the corresponding wind-sand parameters.

We used Advanced Land Observing Satellite (ALOS; launched in 2006) satellite phased array L-band synthetic aperture radar (PALSAR)
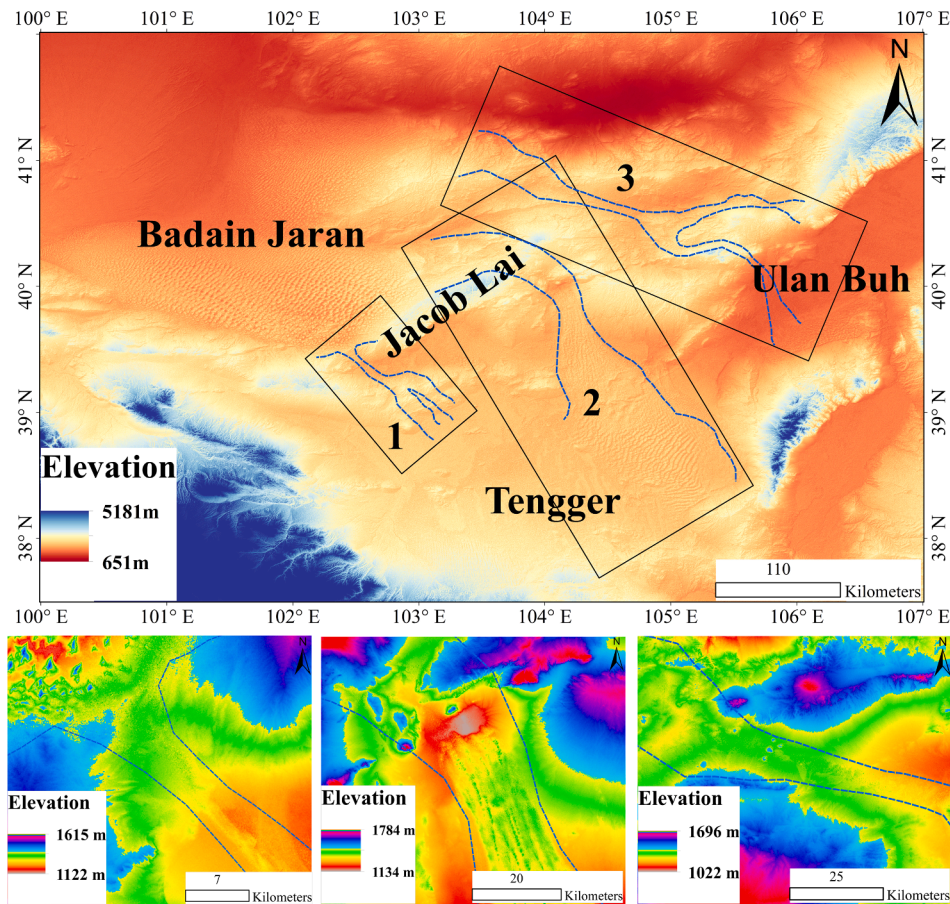
Fig. 2. Elevation distribution over study area. Blue dashed lines represent locations of the sand flow channels. Panels (a), (b), and (c) show the elevation of each channel. (For interpretation of the references to colour in this figure legend, the reader is referred to the web version of this article.)

to collect elevation data. This sensor has three observation modes: high-resolution, scanning synthetic aperture radar, and polarization. The horizontal and vertical accuracies of the data can reach 12.5 m.

2.3. Methods

2.3.1. Average annual sediment transport flux (Q) and resultant average annual sediment transport flux (Q_R)

Here, we only used the complete time series from the 10 m wind data for the latitudinal and longitudinal components.

According to the ERA5 dataset, we calculated the wind speed, u_i, and the direction, $\vec{x_i}$, at different times, for $t_1 \leq t_i \leq t_{N_{obs}}$, $i \in [1;N_{obs}]$. For each time step, i, the shear velocity was computed as follows:

$$u_*^i = \frac{u_i k}{\log(z/z_0)}, \tag{1}$$

where $z = 10$ m is the height of the wind data, $z_0 = 10^{-3} m$ is the characteristic surface roughness, and $k = 0.4$ is the von Karman constant. The threshold velocity u_{*c} was determined according to the following formula proposed by Iversen and Rasmussen (1999):

$$u_{*c} = 0.1 \sqrt{\frac{\rho_s}{\rho_f} gd}, \tag{2}$$

where the gravitational acceleration, g, is 9.81 ms^{-2}, $\rho_s = 2.55 \times 10^3 \ kg/m^3$, $\rho_f = 1.293 \times 10^3 \ kg/m^3$, and the grain diameter, d, is 180 μm. These parameters are generally the global average values. In a given scope, Resultant drift direction (RDD) is less dependent on the grain size and aerodynamic roughness. We selected the global average grain

diameter. The sand-driving wind speed, $u_{*c} \approx 0.19$ ms^{-1}, was obtained at a height of 10 m above the ground.

Many sand transport relationships have been obtained via wind-tunnel experiments, both analytical and phenomenological (Bagnold, 1941; Owen, 1964; Lettau and Lettau, 1977; Ungar and Haff, 1987; Iversen and Rasmussen, 1999; Andreotti, 2004; Sørensen, 2004; Durán and Herrmann, 2006; Durán et al., 2012; Sherman and Li, 2012). In all these relations the sand flux increases with u_*, and there is a threshold wind shear velocity u_{*c} above which the wind can transport grains. They mainly differ by their scaling in u_* and $(u_* - u_{*c})$. Durán et al. (2012), Andreotti (2004) and Ho et al. (2011) have shown from numerical simulations and wind tunnel experiments that the saturated sand flux, i. e., the sand flux at equilibrium over a flat sand bed, scales as $(u_*^2 - u_{*c}^2)$ for small u_* (when $u_* \lesssim 5 \ u_{*c}$) and as u_*^3 for higher u_* values. Most transport laws do scale with u_*^3 for high u_* as suggested by Bagnold (1941). However, the wind velocity values we consider rarely overpass 5 u_{*c}. In this range of wind velocities, wind tunnel data from Iversen and Rasmussen (1999) find a good agreement with the relation proposed by Ungar & Haff (1987), calibrated by Durán et al. (2012). After a series of tests, Ungar and Haff (1987) proposed such a relationship:

$$q = 25 \frac{\rho_f}{\rho_S} \sqrt{\frac{d}{g}} \left(u_*^2 - u_{*c}^2 \right), \tag{3}$$

where ρ_s is the density of sand, and ρ_f is the density of air. Equation (3) can be used to calculate q which is the sediment transport per unit width of a saturated volume.

Next, we calculated the saturated sand flux on a flat sand bed for each time step, as follows:
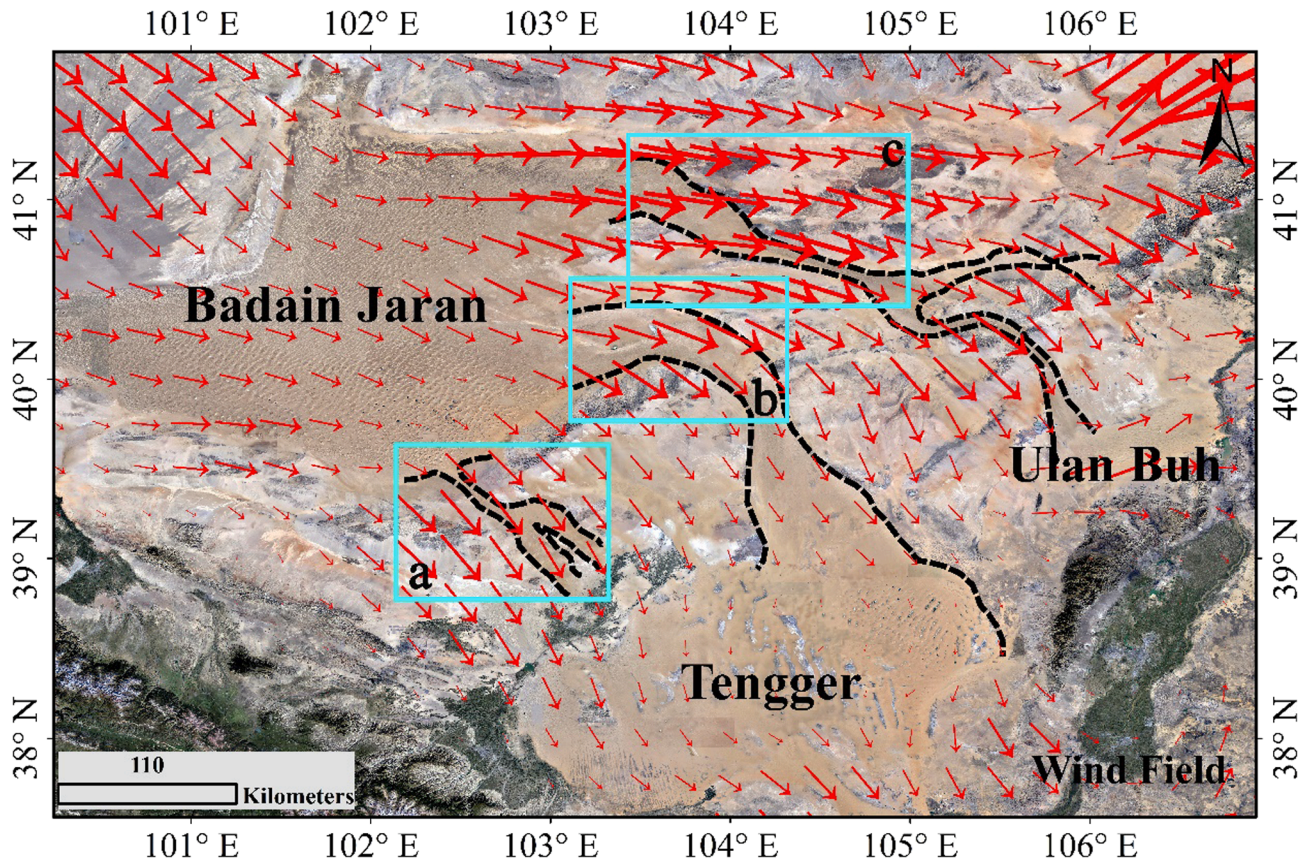
Fig. 3. Resultant average annual sediment transport flux (Q_R)and Resultant drift direction (*RDD*) across study area from 1979 to 2019, based on ERA5 wind data at 10 m. Sizes of red arrows represent Q_R, while arrow directions represent *RDD*. (For interpretation of the references to colour in this figure legend, the reader is referred to the web version of this article.)

$$\overrightarrow{q_i} = \begin{cases} q_i \overrightarrow{x_i}, \ for \ u_*^i \geq u_c, \\ 0, \ for \ u_*^i < u_c, \end{cases} \tag{4}$$

where $q_i = q \ (u_* = u_*^i)$, using Eqs. (1)–(3).

According to each saturated sand flux vector, $\overrightarrow{q_i}$, the average annual sediment transport flux, can be estimated as follows for a flat erodible bed:

$$Q = \frac{\sum_{i=2}^{N_{obs}} \|\overrightarrow{q_i}\|(t_i - t_{i-1})}{\sum_{i=2}^{N_{obs}} (t_i - t_{i-1})}. \tag{5}$$

This quantity does not consider the directionality of sand transport over the entire period (Simmons et al., 1989). Therefore, it is essential to calculate the resultant average annual sediment transport flux, Q_R, which can be calculated as follows:

$$Q_R = \frac{\|\sum_{i=2}^{N_{obs}} \overrightarrow{q_i}(t_i - t_{i-1})\|}{\sum_{i=2}^{N_{obs}} (t_i - t_{i-1})} \tag{6}$$

Q_R is strongly depends on the wind direction. As a dimensionless parameter, the Q_R/Q ratio is an essential indicator of changes in wind regimes (Pearce and Walker, 2005; Tsoar, 2005). $Q_R/Q \rightarrow 1$ indicates that sediment transport tends to be unidirectional. $Q_R/Q \rightarrow 0$ means that most conveying components cancel each other out.

Here, we follow the work of Courrech du Pont et al. (2014) and Gao et al. (2015). We consider that this definition of Q and Q_R is more physical and has the physical unit, and is similar as the widely used *DP* and *RDP* with a unit of VU (Fryberger and Dean, 1979). However, in order to distinguish the traditional *DP* calculated by Fryberger and Dean (1979), we modified the indexes to better express the physical meaning in the current work.

2.3.2. Bed instability and elongation modes

Based on flume experiments and theoretical analyses, previous studies have proposed two dune development modes, depending on variations in the sand supply quantity (Courrech du Pont et al., 2014). These variations are directly manifested as differences in dune orientation and shape (Taniguchi et al., 2012; Parteli et al., 2014; Gao et al., 2015; Lü et al., 2017).

With an abundant sand source, dunes will mainly increase in height; this is known as the dune bed instability mode. In this mode, dunes will be oriented in the direction of maximum vertical synthetic sand transport. When sand sources are scarce and the bed is non-erodible, however, dunes will develop along the direction of synthetic sand transport by extension (this is referred to as the elongation mode). When a dune develops from a fixed sedimentary source, and the angle between the primary and secondary winds, θ, is $> \pi/2$, fingerlike elongations have been observed in dunes. Therefore, if the sand source is fixed, the strike of the resulting dunes should be consistent with the synthetic sand transport direction.

3. Results

3.1. Topography

The study area is located in the eastern and southern mountain basins of the Alxa Plateau, and has a complex topographic structure. The Jacob Lai Mountains separate the Badain Jaran and Tengger Deserts. We identified a topographical height transition area between the southwest edge of Jacob Lai Mountain and the southeast region of the Great Northern Mountains, which is where the first sand flow channel is located (Fig. 2a). This channel is the smallest of the three and the richest
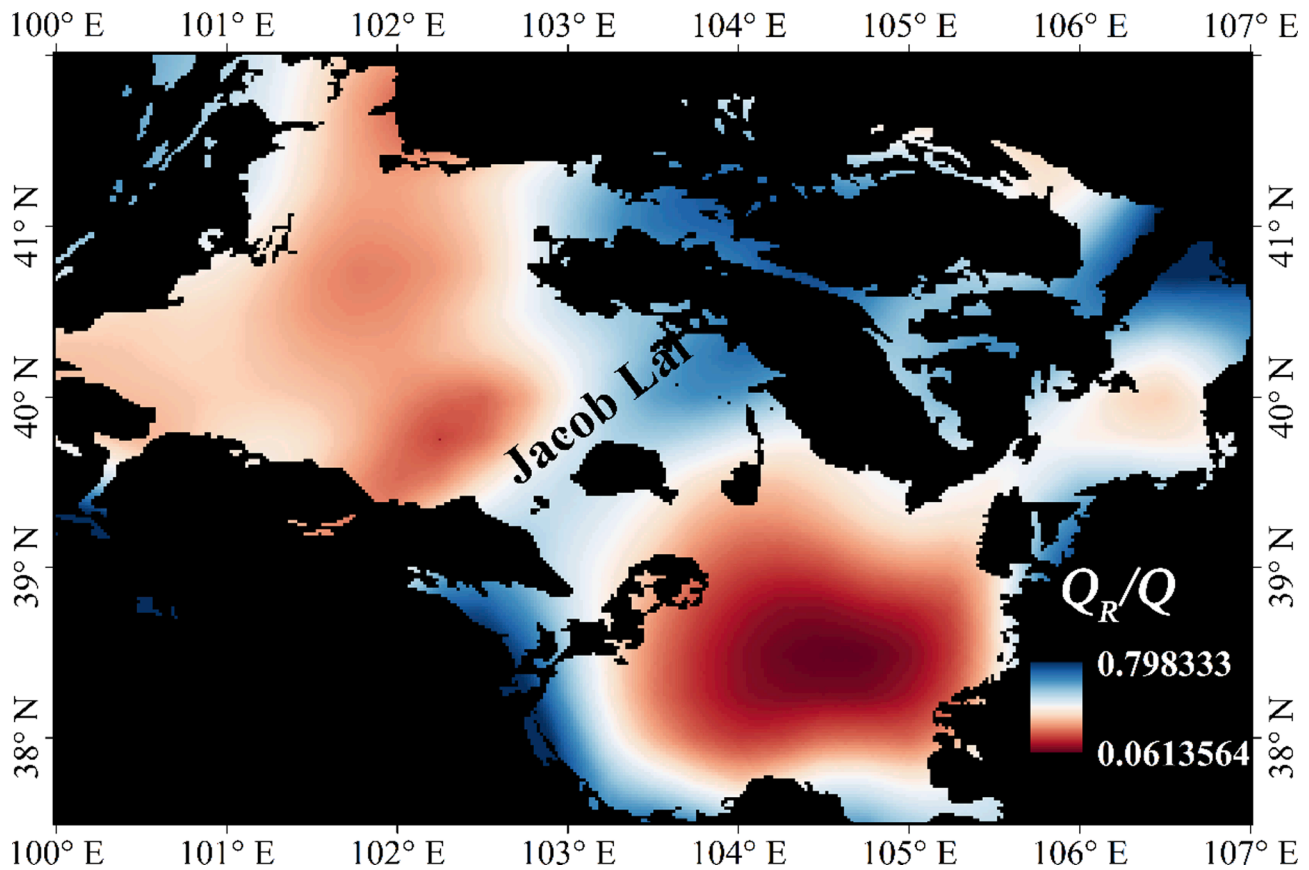
Fig. 4. Spatial pattern of wind directional variability (Q_R/Q) in study area (1979–2019). Standard kriging interpolation method was used to generate graph based on ERA5 wind data at 10 m.

in geomorphic types. We found that the valleys in the northeast of Jacob Lai Mountain are filled with sand, and are connected with the Tengger Desert under the promotion of prevailing winds, thus forming a second sand flow channel (Fig. 2b). Compared with the other two channels, the terrain fluctuation of this channel is larger, but it is generally lower than the mountain height on both sides. We also found another channel between the Zongnai Mountain and the bedrock hills in the northeastern region of the Badain Jaran Desert. This channel continues southeast, crossing the lower southwest margin of the Yinshan Mountains and connecting with the Ulan Buh Desert (Fig. 2c). As shown in Fig. 2, these three channels have noticeable elevation differences, which provide favorable terrain conditions for the transportation of sand.

3.2. Wind regime

3.2.1. Resultant average annual sediment transport flux (Q_R) and resultant drift direction (RDD)

Aeolian geomorphology cannot be shaped without the influence of wind (Bagnold, 1941; Pye and Tsoar, 1990; Lancaster, 1995). Within channels, wind power is particularly prominent due to the venturi effect. We calculated the Q_R and *RDD* for the entire study area using ERA5 reanalysis wind data at a height of 10 m, from the complete 41-yr time series (1979–2019; Fig. 3). We found that the entire study area was affected by westerly and northwest winds during this period, with sediment transport being focused in west-east or northwest-southeast orientations. In particular, the channels exhibited relatively high resultant drift potential, indicating that their sediment transport activities are intense and concentrated.

3.2.2. Distribution of wind directional variability

The rate of wind directional variability (Q_R/Q) is an essential

indicator of wind regimes. When wind originates from one direction, Q_R/Q will be approximately 1. In contrast, when wind creates multiple orders, Q_R/Q will be approximately 0. We calculated the spatial distribution of the wind directional variability by spatial interpolation, using Q and Q_R (Fig. 4). Our results show that Q_R/Q in the desert was small, and that the wind directional variability was large. We found that dune development was more complex with respect to blunt bimodal wind regimes or compound wind regimes. In the sand flow channels, Q_R/Q was relatively large, and the wind directional variability was slight. Thus, this narrow single-peak wind regime promoted the formation and development of simple dunes.

3.3. Dune distribution in channels

Wind conditions and sand source abundance are two critical factors that influence dune topography (Bao et al., 2015). Area-based differences in dune morphology are a visual representation of wind conditions and sand source availability. Here, combined with satellite images, we used the vectorization method to outline the shape of dunes in the channels; we found that the forms of dunes in the channel were relatively simple. Moreover, in channels b and c, we identified a transition landscape from barchan dunes to barchan dune chains, then to transverse dunes (including barchan dunes) (Fig. 5).

In areas with relatively few upwind sand sources, barchan dunes are often affected by a single wind condition. As the topography rises, sand particles accumulate along the resultant drift direction. Thus, barchan dunes become connected into pieces, gradually forming a barchan dune chain, and then transverse dunes (including barchan dunes). We therefore determined that there was a dune type transition area in the direction of sand transport. The spatial oscillation behavior was magnified by elevation (Gadal et al., 2020), and apparent changes in the
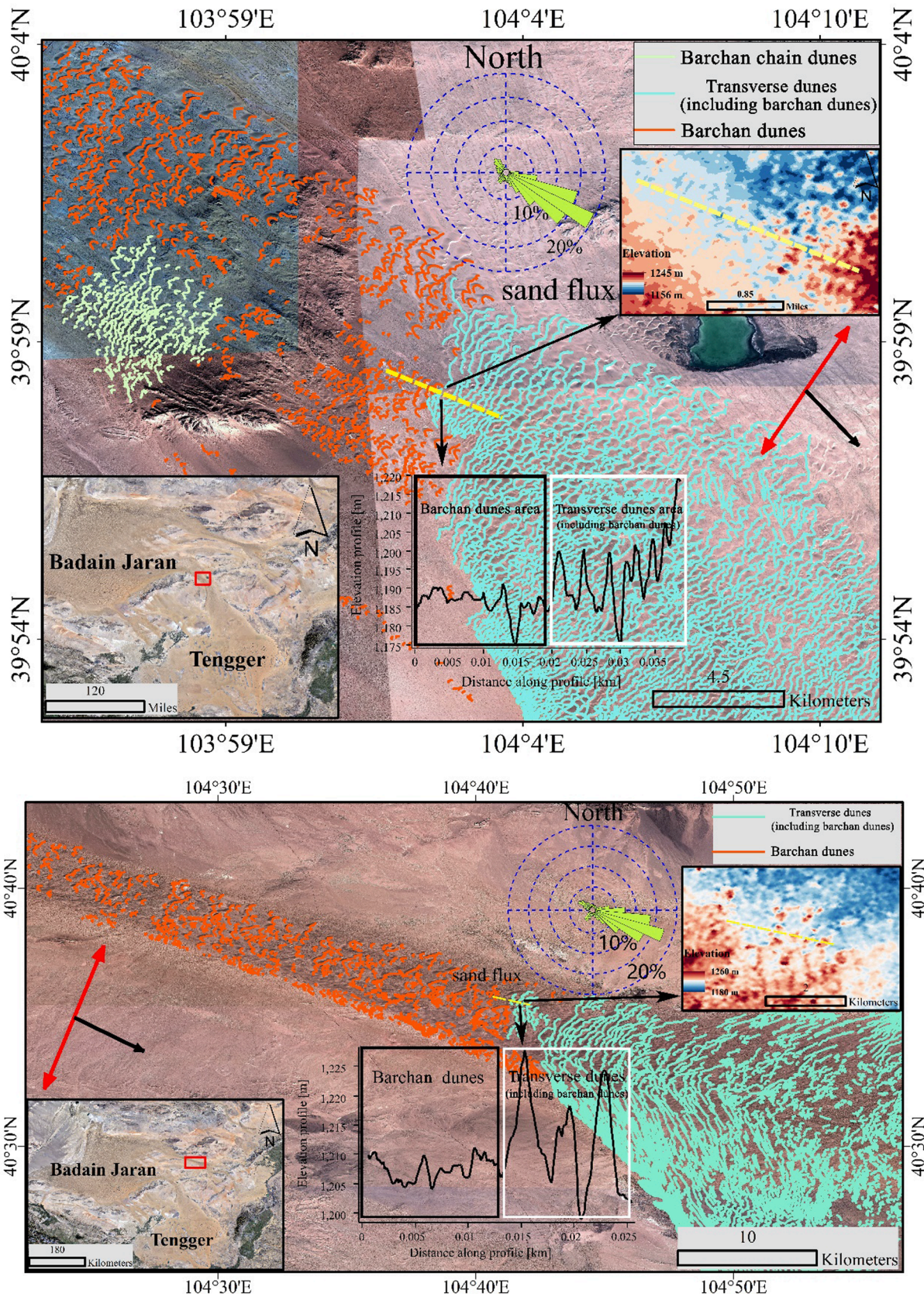
Fig. 5. Dune distribution and transition landscape in sand flow channels b and c. Sand flux roses indicate direction of sand transport. Yellow dotted line shows transition area of selected dune type. Red bidirectional arrows represent bed instability mode. Black unidirectional arrows represent elongation mode. The black curve shows the spatial variation trend of elevation in the yellow transition region. (For interpretation of the references to colour in this figure legend, the reader is referred to the web version of this article.)
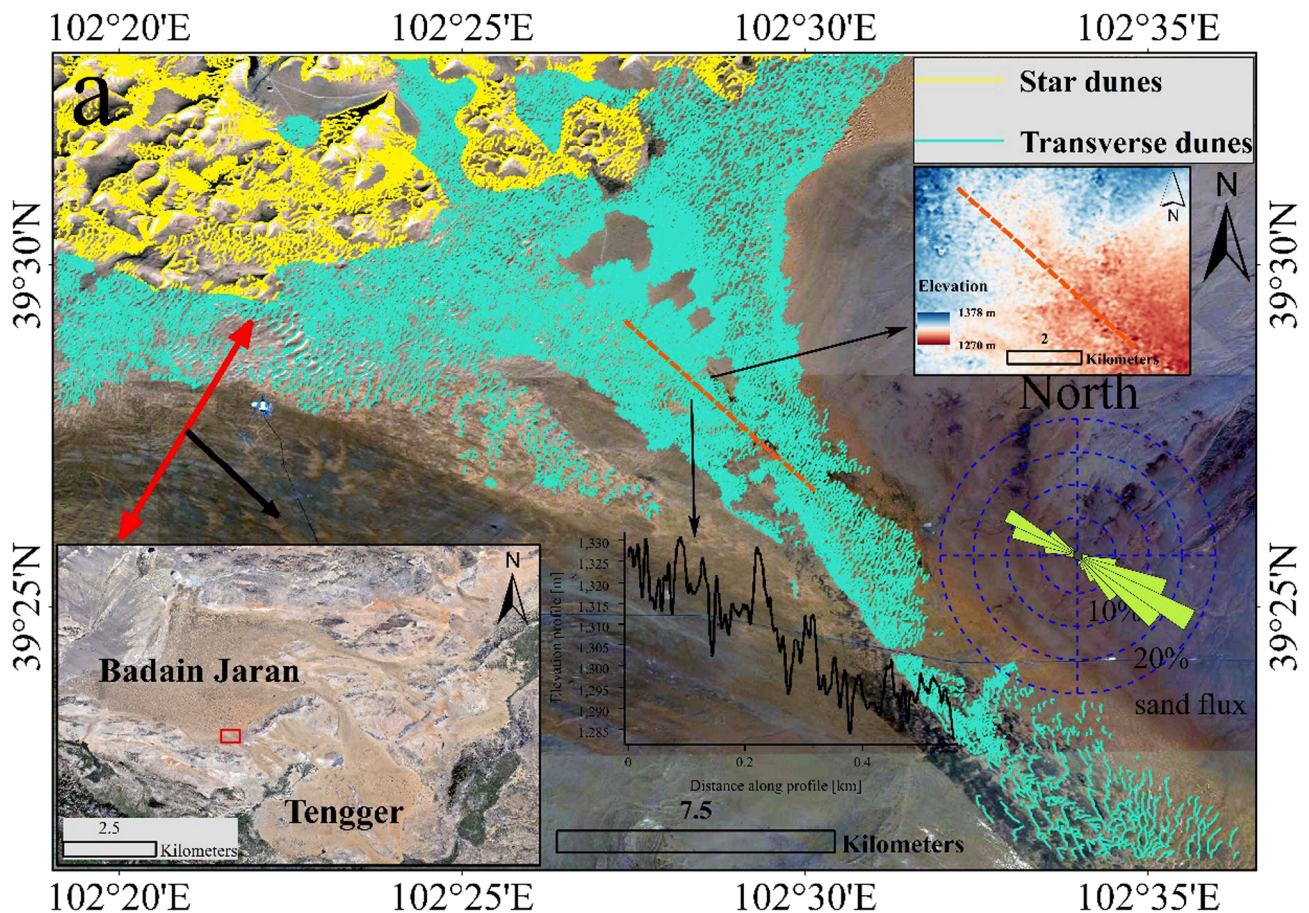
Fig. 6. Dune distribution and transition landscape within sand flow channel a. Sand flux rose indicates direction of sand transport. Orange dotted line shows the area of variation in transverse dune elevation. Red bidirectional arrows represent bed instability mode. Black unidirectional arrows represent elongation mode. (For interpretation of the references to colour in this figure legend, the reader is referred to the web version of this article.)

wavelengths of the dunes could be seen.

Moreover, we observed that the trend of the dunes was basically aligned along the resultant drift direction, as predicted by the unstable mode of the bed surface developed by the dunes. The formation, development, and evolution of dunes are affected by many factors; therefore, the effects of the channels on dune formation do not rule out the presence of complex dunes. These complex dunes can form when the stability of the transverse dunes is broken.

The sand flow channel c is relatively particular in that it extends to the north of Minqin (Fig. 6). Its entrance is located at the southwest edge of the Badain Jaran Desert, its sand source is abundant, and we found that the wind conditions within this channel were relatively complex. The channel exhibited a very obvious reverse wind regime, as evidenced by the dominance of transverse dunes, but the overall direction of sand transport still extended along the channel to the southeast. There is a significant topographic drop from the edge of the desert to the inside of the channel, with a corresponding decrease in dune height. This channel is dominated by transverse dunes with a local distribution of barchan dune chains. The landform types within the corridor are relatively complex, with sandy, saline, and grassland areas (Liu et al., 2011). Transitional human reclamation, in addition to transitional grazing, has accelerated the process of desertification in this corridor, leading to frequent sand and dust storms in Minqin.

3.4. Dune movement

Dune movement refers to the distance that a dune moves due to wind. This process occurs due to erosion occurring over the windward

slope and accumulation occurring over the leeward slope (Li et al., 2021). Here, we measured dune movement in the studied channels using two phases of historical remote sensing imagery, obtained from Google Earth. We selected barchan dunes and transverse dunes (including barchan dunes) in channel b (Fig. 7). First, we outlined each dune, and then we chose the two wings of the dune and the middle of its ridgeline as measuring points. We then measured the distances traveled by these three points during the study interval and calculated the average distance. Finally, we calculated the moving speed of the dune, according to the time interval between the two images and the distance moved by the dune (Li et al., 2021). Our results show that the dunes in the channels moved significantly faster. In particular, we found that barchan dunes moved at speeds up to 27 m·yr^{-1}. The dunes moved substantially slower in the transverse dune area.

4. Discussion

4.1. Mode of action by which sand flow channels affect desert landscapes

Studying the roles of sand flow channels in desert landscapes requires an exploration of the contrasting sediment characteristics between different deserts connected by channels, from a physical source perspective. Taking the Badain Jaran and Tengger Deserts as examples, Li (2011) conducted a detailed study into the sediment characteristics of the two deserts in terms of sediment grain size, mineral composition, and geochemical elements. They found that the grain size compositions of the two deserts were very similar, for both surface and vertical sediments. The light and heavy mineral types in the surface sediments were
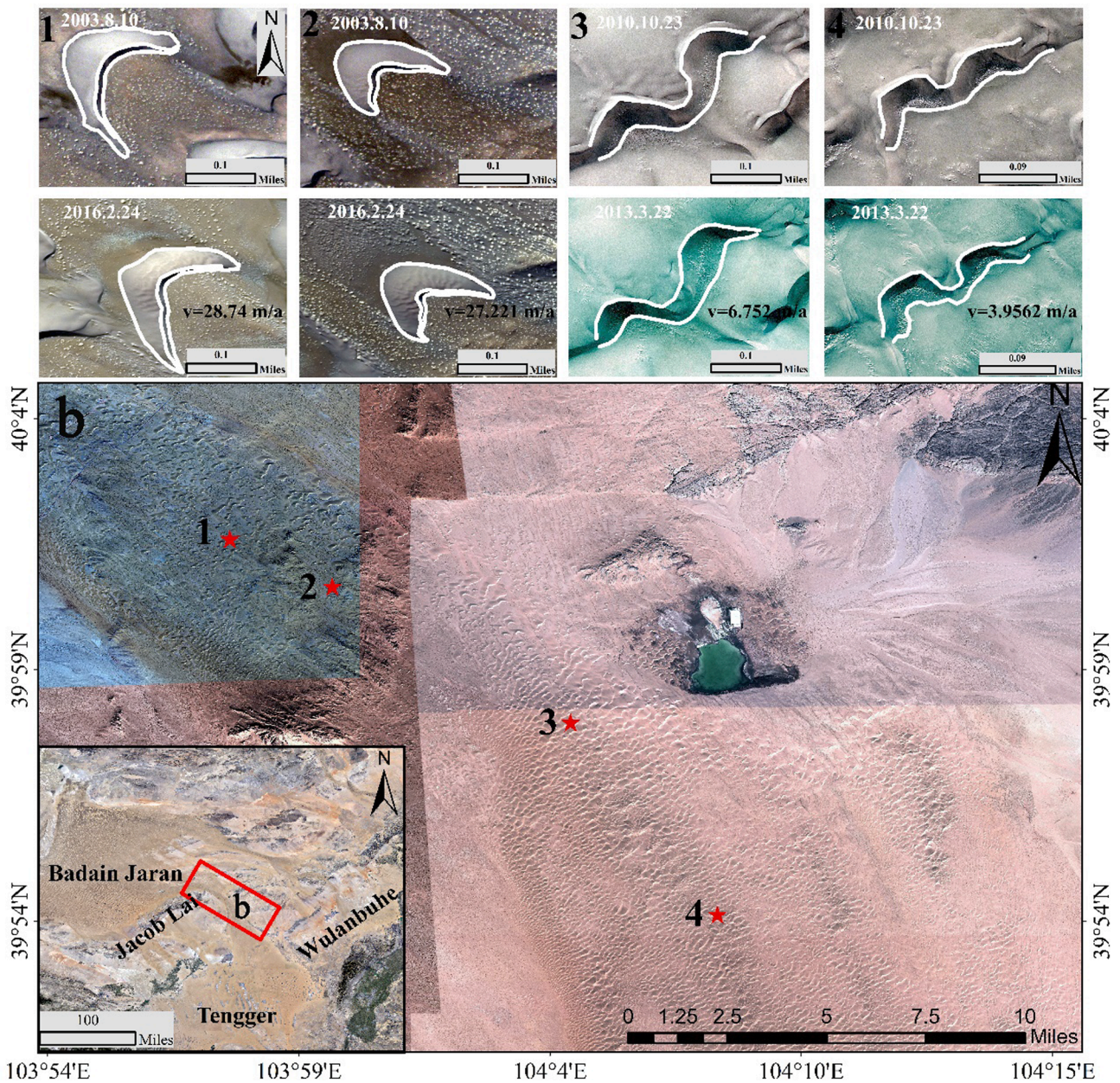
Fig. 7. Dune movement speeds within sand flow channel b. Red stars represent locations of selected dunes. (For interpretation of the references to colour in this figure legend, the reader is referred to the web version of this article.)

the same, but their specific gravities differed slightly. SiO_2 and Al_2O_3 dominated the macronutrients in the geochemical elements, while Ba was dominant in the trace elements. Although Li (2011) observed some differences in the particle size parameters and mineral-specific gravities of these two deserts, their overall material origins were very close. Therefore, as a geomorphic landscape connecting these two independent deserts, we believe that the sand flow channels in this area act as a direct sand recharge channel between them.

4.2. Sand flow channels in other deserts

Satellite imagery observations show that different channel landscapes exist in many desert landscapes globally. For example, we have identified several such channels, which lies between the Mazartagh, Gudong, and Luositagh Mountains in the Taklamakan Desert (Fig. 8a). These channels developed in the interior of a separate geomorphic unit, in the Taklamakan Desert. They connect the north and south of the

mountain range and form coherent transverse dunes, in contrast to the dune morphologies observed on the windward and leeward slopes of the mountain range. We have also found a large spatial scale "wind gap" in the Tibesti Mountains of the Sahara Desert in North Africa and the Massif to the southeast (Fig. 8b); this represents another form of sand flow channel. Based on the two wings of the barchan dunes and the trends of many Yardang landform erosion areas, we can infer that the direction of aeolian sand flow in this channel is northeast-southwest. We believe that a large portion of the sand from northeastern Sahara is being transported downwind through the channel, which presents a significant challenge for sand control efforts in southern North Africa. The Ad-Dahna Desert in the Arabian Peninsula, which lies close to the Arabian Nubian shield and east of the Persian Gulf, has become a desert corridor connecting the An-Nafud and Rubal-Khali Deserts; this represents a third form of sand flow channel (Fig. 8c). Low-pressure circulation over the Indian subcontinent mainly affects the Arabian Peninsula in summer, while the Sahara High in North Africa affects the Arabian Peninsula in
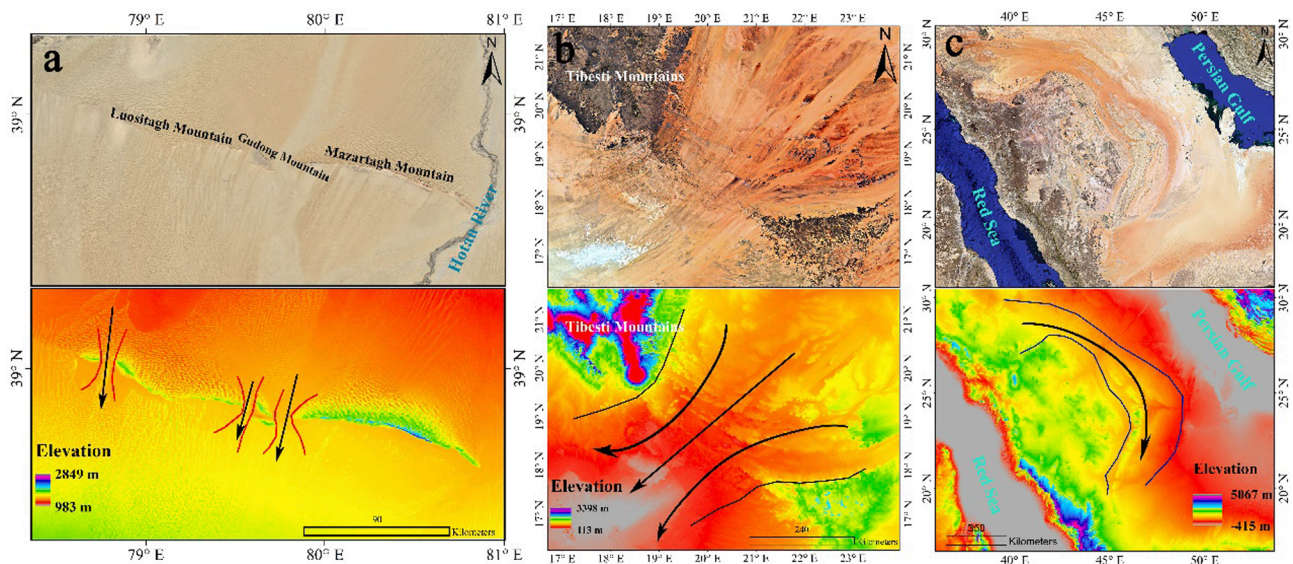
Fig. 8. Other forms of sand flow channels. Satellite images and elevation maps of (a) Mazartagh and Luositagh Mountains, (b) Massif region southeast of Tibesti Mountains, and (c) Arabian Peninsula region. Black arrows represent directions of sand transport in sand flow channels.

winter. Therefore, this region is primarily controlled by northwest winds in spring and summer and south-southwest winds in winter (Yang et al., 2008). This results in the transport of fluvial sand from the upwind An-Nafud Desert to the Ad-Dahna Desert, bringing an abundant source of sand to the downwind Rubal-Khali Desert. Thus, sand flow channels are diverse; their formation and development mechanisms can vary, so future research should aim to study various types of sand flow channels.

5. Conclusions

Here, we analyzed three sand flow channels located in the Badain Jaran, Tengger, and Ulan Buh Deserts. We found that these sand flow channels were generally located in low areas between two mountains or bedrock hills, or in regions where mountains were present in a valley area. We identified that sand was carried into these channels and deposited through the prevailing wind transport, thereby gradually forming a channel landform landscape dominated by wind camp force terrain. There are other forms of sand flow channels, such as the large spatial scale sand flow channels that have formed between plateaus in the Sahara Desert, and those that have formed in the Arabian Peninsula, which only have mountainous terrain on one side.

Under the influence of prevailing west and northwest winds, we found that the direction of resultant drift direction across the entire study area was generally west-east or northwest-southeast during the study interval. Owing to the venturi effect caused by the terrain, the airflow accelerated when flowing through the studied channels, with the resulting high winds leading to a strong sand transport capacity and fast-moving dunes. Moreover, the wind direction variability was low, indicating that the wind conditions in these channels were unimodal. Influenced by this unimodal wind condition, the dune types in the channels were relatively simple; they were dominated by barchan and transverse dunes (including barchan dunes). We also identified a transitional landscape comprising the transition of barchan dunes to transverse (including barchan dunes) or complex dunes.

Comparing sediment characteristics and the of prevailing wind directions revealed that sand transport through these channels provided a direct source of sand recharge to the Tengger and Ulan Buh Deserts while promoting the formation and evolution of downwind desert areas. The sand flow channels that we identified currently connect three deserts into a complete desert system, shaping the area's unique geomorphological landscape. Therefore, three deserts are collectively called Alxa Desert in China.

Here we analyzed the shaping effects and influences of sand flow channels on desert landscapes from a geomorphological perspective, but our study lacked any in-depth mechanistic research. A deeper analysis of the sand flow channels would be an exciting research direction. It is essential to understand the formation of desert systems to ensure the success of human sand control and management practices.

Declaration of Competing Interest

The authors declare that they have no known competing financial interests or personal relationships that could have appeared to influence the work reported in this paper.

References

Andreotti, B., 2004. A two-species model of aeolian sand transport. J. Fluid Mech. 510, 47–70.

Bao, F., Dong, Z., Zhang, Z., 2015. Wind regime in the Qaidam Basin desert. J. Desert Res. 35 (3), 549–554.

Bullard, J.E., McTainsh, G.H., 2003. Aeolian-fluvial interactions in dryland environments: examples, concepts and Australia case study. Prog. Phys. Geogr. 27 (4), 471–501.

Courrech du Pont, S., Narteau, C., Gao, X., 2014. Two modes for dune orientation. Geology. 42 (9), 743–746.

Chun, X., Chen, F., Fan, Y., et al., 2007. Formation of Ulan Buh Desert and its environmental evolution. J. Desert Res. 27 (6), 927–931.

Durán, O., Claudin, P., Andreotti, B., 2012. On aeolian transport: grain-scale interactions, dynamical mechanisms and scaling laws. Aeolian Res. 3 (3), 243–270.

Durán, O., Herrmann, H., 2006. Modelling of saturated sand flux. JSTAT. 2006 (07), P07011.

Durán, O., Claudin, P., Andreotti, B., 2012. On aeolian transport: grain-scale interactions, dynamical mechanisms and scaling laws. Aeolian Res. 3 (3), 243–270.

Draut, A.E., 2012. Effects of river regulation on aeolian landscapes, Colorado River, southwestern USA. J. Geophys. Res. Earth Surf. 117 (F2).

Bagnold, R.A., 1941. The Physics of Blown Sand and Desert Dunes. Springer, Netherlands.

Fedorovich, 1962. The Origin of Desert Landscapes and its Research Methods. Science Press.

Fryberger, S.G., Dean, G., 1979. Dune forms and wind regime. In: A Study of Global Sand Seas. US Government Printing Office Washington, vol. 1052, pp. 137–169.

Gao, X., Narteau, C., Rozier, O., Courrech du Pont, S., 2015. Phase diagram of dune shape and orientation depending on sand availability. Sci. Rep. 5, 14677.

Gadal, C., Narteau, C., Ewing, R.C., Gunn, A., Jerolmack, D., Andreotti, B., Claudin, P., 2020. Spatial and temporal development of incipient dunes. Geophys. Res. Lett. 47 e2020GL088919.

Gao, X., Narteau, C., Gadal, C., 2021. Migration of reversing dunes against the sand flow channel as a singular expression of the speed-up effect. J. Geophys. Res. Earth Surf. 126.

Ho, T.D., Valance, A., Dupont, P., Ould El Moctar, A., 2011. Scaling laws in aeolian sand transport. Phys. Rev. Lett. 106, 265–270.

Iversen, J.D., Rasmussen, K.R., 1999. The effect of wind speed and bed slope on sand transport. Sedimentology. 46 (4), 723–731.

Jin, H., Dong, G., 2001. Preliminary study on the role of river wriggling in the evolution of Aeolian landforms in arid area-taking Hotan river as an example. J. Desert Res. 021 (004), 367–373.

Lancaster, N., 1995. Geomorphology of Desert Dunes. Routledge, London, 290 pp.

Lettau, K., Lettau, H., 1977. Experimental and micrometeorological field studies of dune migration. In: Lettau, K., Lettau, H. (Eds), Exploring the World's Driest Climate, University of Wisconsin Press, Madison.

Li, E., 2011. A Comparative Study of Sediment Characteristics in the Badain Jaran and Tengger Deserts. Shaanxi Normal University.

Li, X., Chen, F., Li, X., et al., 2006. Research situation, problems and significances on transverse mega-dunes in Badain Jaran Desert. J. Desert Res. 26 (6), 880–884.

Li, J., et al., 2021. Spatial areaalization and response to morphological parameters of dune migration in the Qaidam Basin of China. Trans. Chin. Soc. Agric. Eng. 37, 7.

Liu, Y., Wang, X., Zhang, X., et al., 2011. Desertification Process and Its Driving Forces in the Dune-activation Area between the Badain Juran and Tengger Deserts. Arid Zone Res. 28 (6), 957–966.

Lü, P., Narteau, C., Dong, Z., Rozier, O., Courrech du Pont, S., 2017. Unravelling raked linear dunes to explain the coexistence of bedforms in complex dune fields. Nat. Comms. 8, 14239.

Meng, X., Guo, J., Han, Y., 2018. Preliminarily assessment of ERA5 reanalysis data. J. Marine Meteorol. 38 (1), 91–99.

Olauson, J., 2018. Era5: the new champion of wind power modelling? Renewable Energy. 126, 322–331.

Owen, P.R., 1964. Saltation of uniform grains in air. J. Fluid Mech. 20 (2), 225–242.

Pye, K., Tsoar, H., 1990. Aeolian Sand and Sand Dunes. Springer, Netherlands, pp. 416.

Parteli, E.J.R., Durán, O., Bourke, M.C., Tsoar, H., Pöschel, T., Herrmann, H., 2014. Origins of barchan dune asymmetry: insights from numerical simulations. Aeolian Res. 12, 121–133.

Pearce, K.I., Walker, I.J., 2005. Frequency and magnitude biases in the 'Fryberger' model, with implications for characterizing geomorphically effective winds. Geomorphology. 68 (1–2), 39–55.

Schwarz, C., van Starrenburg, C., Donker, J., Ruessink, G., 2021. Wind and sand transport across a vegetated foredune slope. J. Geophys. Res.: Earth Surf. 126 (1) e2020JF005732.

Sherman, D.J., Li, B., 2012. Predicting aeolian sand transport rates: a reevaluation of models. Aeolian Res. 3 (4), 371–378.

Simmons, A., Uppala, S., Dee, D., Kobayashi, S., 1989. ERA-Interim: New ECMWF reanalysis products from 1989 onwards. ECMWF Newsletter. 110, 25–35.

Sørensen, M., 2004. On the rate of aeolian sand transport. Geomorphology. 59 (1–4), 53–62.

Taniguchi, K., Endo, N., Sekiguchi, H., 2012. The effect of periodic changes in wind direction on the deformation and morphology of isolated sand dunes based on flume experiments and field data from the Western Sahara. Geomorphology. 179, 286–299.

Tsoar, H., 2005. Sand dunes mobility and stability in relation to climate. Phys. A. 357 (1), 50–56.

Ungar, J.E., Haff, P.K., 1987. Steady state saltation in air. Sedimentology. 34 (2), 289–299.

Wilson, I.G., 1971. Desert sandflow basins and a model for the development of ergs. Geogr. J. 137 (2), 180.

Yang, X., Qing, H., Chen, X., 2008. The characteristics and causes of the Rub Al Khali desert. Desert & Oasis Meteorol. 002 (002), 53–57.

Yang, Y., Lu, J., 1990. The formation of Mt. maza-tage in the Taklamakan desert and its geographical significance. Geograph. Res. 9 (003), 24–32.

Yan, P., Li, X., Ma, Y., Wu, W., Qian, Y., 2015. Morphological characteristics of interactions between deserts and rivers in northern China. Aeolian Res. 19, 225–233.

Zhu, Z., 1980. The General Induction to Chinese Desert. Science Press, Beijing, China, 107 pp.

Zu, R., Zhang, K., Qu, J., et al., 2005. Characteristics of surface winds takla-makan deserts and their relationship to the orientation of dunes in neighboring areas. J. Appl. Meteorol. 16 (4), 8.